Exergy analysis and particle swarm optimization of clean energy router based on a solar-thermal-assisted advanced adiabatic compressed air energy storage system

Ni, Chenyixuan; Chen, Laijun; Chen, Xiaotao; Zhai, Junyi; Mei, Shengwei; Zhang, Xiao-Ping

DOI:
10.1049/rpg2.12758

Document Version
Publisher's PDF, also known as Version of record

Citation for published version (Harvard):
Ni, C, Chen, L, Chen, X, Zhai, J, Mei, S & Zhang, XP 2023, 'Exergy analysis and particle swarm optimization of clean energy router based on a solar-thermal-assisted advanced adiabatic compressed air energy storage system', *IET Renewable Power Generation*, vol. 17, no. 9, pp. 2302-2314. https://doi.org/10.1049/rpg2.12758

Received: 9 August 2022 | Revised: 20 March 2023 | Accepted: 10 May 2023

IET Renewable Power Generation

DOI: 10.1049/rpg2.12758

The Institution of Engineering and Technology WILEY

ORIGINAL RESEARCH

Exergy analysis and particle swarm optimization of clean energy router based on a solar-thermal-assisted advanced adiabatic compressed air energy storage system

Chenyixuan Ni[1] | **Laijun Chen**[2] | **Xiaotao Chen**[2] | **Junyi Zhai**[3] | **Shengwei Mei**[2] | **Xiao-Ping Zhang**[1]

[1]EESE Department, School of Engineering, University of Birmingham, Edgbastion, Birmingham, UK

[2]Qinghai Key Lab of Efficient Utilization of Clean Energy (New Energy Photovoltaic Industry Research Center), Qinghai University, Xining, People's Republic of China

[3]The College of New Energy, China University of Petroleum (East China), Qingdao, People's Republic of China

Correspondence
Xiaotao Chen, Qinghai Key Lab of Efficient Utilization of Clean Energy (New Energy Photovoltaic Industry Research Center), Qinghai University, Xining 810016, People's Republic of China.
Email: chenxiaotao@qhu.edu.cn

Xiao-Ping Zhang, EESE Department, School of Engineering, University of Birmingham, Edgbastion B15 2TT Birmingham, UK.
Email: x.p.zhang@bham.ac.uk

Funding information
Engineering and Physical Sciences Research Council, Grant/Award Numbers: EP/N032888/1, EP/L017725/1; National Key R&D Program of China, Grant/Award Number: 2020YFD1100500

Abstract

The clean Energy router based on advanced adiabatic compressed air energy storage (AA-CAES) has the characteristics of large capacity, high efficiency and zero carbon emission which are an effective mitigation scheme for the integration of renewables and peak-shaving and a new clean energy technology for storing energy in the world. A novel solar-thermal-assisted AA-CAES (ST-AA-CAES) is proposed in this paper, integrating variable thermal energy storage to improve the system electric to electric (E2E) and round-trip efficiency (RTE). The efficiency and exergy evaluation of ST-AA-CAES are carried out to determine the performance of ST-AA -CAES. The results illustrate that E2E, RTE, and exergy efficiency can reach 56.4%, 95.5%, and 55.9%, respectively. Meanwhile, the details of exergy efficiency and destruction of each subsystem are demonstrated. Particle swarm optimization algorithm is applied to analyse the economy of optimally integrated energy systems which has the advantages of high accuracy, convenient implementation and fast convergence. The system can be applied in abundant solar energy resources area with high efficiency and multi-energy supply capability.

1 | INTRODUCTION

With the current shortage of fossil sources and environmental protection, renewable energy (RE) such as wind energy and solar energy have attracted more and more attention. Due to the rapid development of RE, its characteristics of intermittency and volatility can accompany great challenges to renewable energy sources and power grids [1–3]. During periods of low natural wind, the supply of wind power is insufficient. Similarly, solar power cannot be utilized while the situations of cloud and night. The above reasons demonstrate the impendence of the adjustable ability of the power grid. Energy storage technology (EST) can achieve stable space-time transfer of energy, and it is also one of the effective solutions to realize the new source of fluctuation from the qualitative perspective of the safety and stability of the power grid [4].

The power can be stored through specific mediums and then the stored energy should be released to generate power when the demand for the power grid increases. The electric energy storage system is one of the schemes for large-scale utilization RE, which is an effective approach to improve the efficiency, safety and economy of the conventional power system [5]. At the same time, large-scale energy storage system is a necessary part of smart grid, distributed energy generation and micro-grid technology. The current commercial EST mainly includes pumped hydroelectric storage (PHS), compressed air energy

storage (CAES), battery energy storage (BES) and superconducting magnetic energy storage (SMES) [6]. Among them, PHS and CAES have the characteristics of large capacity, long cycle life and low cost, which have the potential for commercial promotion and application. They are both the key technologies to solving the fluctuating renewable energy grid. Although PHS is a mature and widely used EST, due to the limitations of PHS are abundant water resources and geological conditions, it is difficult to accomplish in cold, arid and light resource-rich areas [7]. Because the surface with abundant light sources needs to be considered for the evaporation of water resources and the source of water resources in arid areas, it will also increase the difficulty and realization of construction. AA-CAES is a kind of use of compressed air to store electric power with the advantages of zero carbon emission and no limitation of geographical locations.

In the meanwhile, some parts of storage tanks can be used by natural caves and underground salt caves instead of the cost of construction. Therefore, it has more commercial application prospects [8]. Compared with the traditional CAES, AA-CAES combine electricity energy storage and TES which can store the heat produced in the compression stage and then the stored thermal energy can be used to preheat the high-pressure air to enhance the efficiency of power generation. Due to the addition of thermal energy storage (TES), the compression heat can be used to improve the efficiency of power generation (the increase of power generation efficiency increased by the outlet temperature of high-pressure air) [9].

To improve the overall efficiency of the system and reduce carbon emissions, literature [10] only use solar energy to heat the inlet air of the turbine to improve power generation efficiency without using compression heat to raise the air temperature. In contrast to the original system, the hybrid CAES system combined with a solar collector was designed in literature [11], which increased the energy conversion efficiency by 25% and reduced the carbon emission by 42%. Because the system used accelerants to improve the power generation efficiency, hydrogen with low carbon emission was used to replace natural gas which generated less pollution. A new method of integrating geothermal and solar energy resources with the CAES system is proposed in the literature [12]. The system combines geothermal and parabolic solar collectors as heat sources with compressed air energy storage for peak balancing and hot water production without any carbon dioxide emissions. Literature [13] studies the impact of solar compressed air energy storage system (SPCAES) as a new type of EST on energy hub (EH) operating performance and efficiency as well as environmental costs and proposes a framework based on typical EH and it shows that EST is an effective approach in reducing operating costs and emissions in energy management. Literature [14] used solar energy to raise the inlet temperature of air turbines and perform technical and economic analysis. Therefore, the above research results indicate that the integration of CAES-TES and renewable energy can improve system efficiency. However, the above research does not fully consider the application of compression heat recovery and the economy and flexibility of the system.

To address the research gap, this paper's contributions are presented as follows:

1. This paper proposes a novel ST-AA-CAES, which utilizes the TES and solar thermal to improve the system efficiency of power generation and round-trip.
2. The high heat collection efficiency of the solar energy with low loss can be implemented in this system to provide a new approach to improve the efficiency of the multi-energy supply based on the verification of the efficiency of exergy and round-trip of the system.
3. Particle swarm optimization algorithm (PSO) is applied for the analysis of the economy of optimally integrated energy systems to verify the economy of the system.

The paper is organised as follows. The description of the ST-AA-CAES system is presented in Section 2. The analysis of exergy efficiency and exergy destruction of all subsystems are provided in Section 3. The details of using PSO to analyse the optimal economic solution of the clean energy router (CER) are outlined in Section 4. The results and discussion are demonstrated in Section 5 and the conclusions are provided in Section 6.

2 | SYSTEM DESCRIPTION

As shown in Figure 1, ST-AA-CAES mainly composes a seven-stage compression and a two-stage expansion to achieve the performance of the system. There are four main subsystems for the system, containing a compressor system (COM), a turbine system (TUR), a molten salt thermal storage (MSTS) and a solar and thermal collection and storage (STC). The COM includes a seven-stage compressor, a seven-stage air intercooler and high-temperature water storage system with a hot water tank (HWT). The design of the compression stage is determined by the maximum operating pressure of the steel pipe tank (SPT) and the kind of compressor used with the maximum design pressure of SPT is 10 MPa. Based on the compressor ratio, the pressure can be achieved to the demand for the design of the COM.

The STC has the function of absorbing heat from solar to preheat the high-pressure air and then MSTS reheat to obtain the requirement of the inlet air temperature. This process ensures the E2E efficiency of the original system and moderately reduces the power consumption of MSTS for preheating high-pressure. There are three main components of the STC, which are a low-temperature oil tank (LOT), high-temperature oil tank (HOT) and a parabolic trough collector (PTC). There is a throttle valve (TV) in TUR which can control the outlet of air mass flow. Two air reheaters are also included which obtain the heat from MSTS. Meanwhile, another two heat exchangers can be used to preheat the air before going through reheaters. Moreover, there are four kinds of fluids are outlined in this system, air flow (AR), water flow (WA), TES medium flow and oil flow (O). All the energy flows and details of the system are listed in Figure 1. Even if the COM, SPT and TUR subsystems

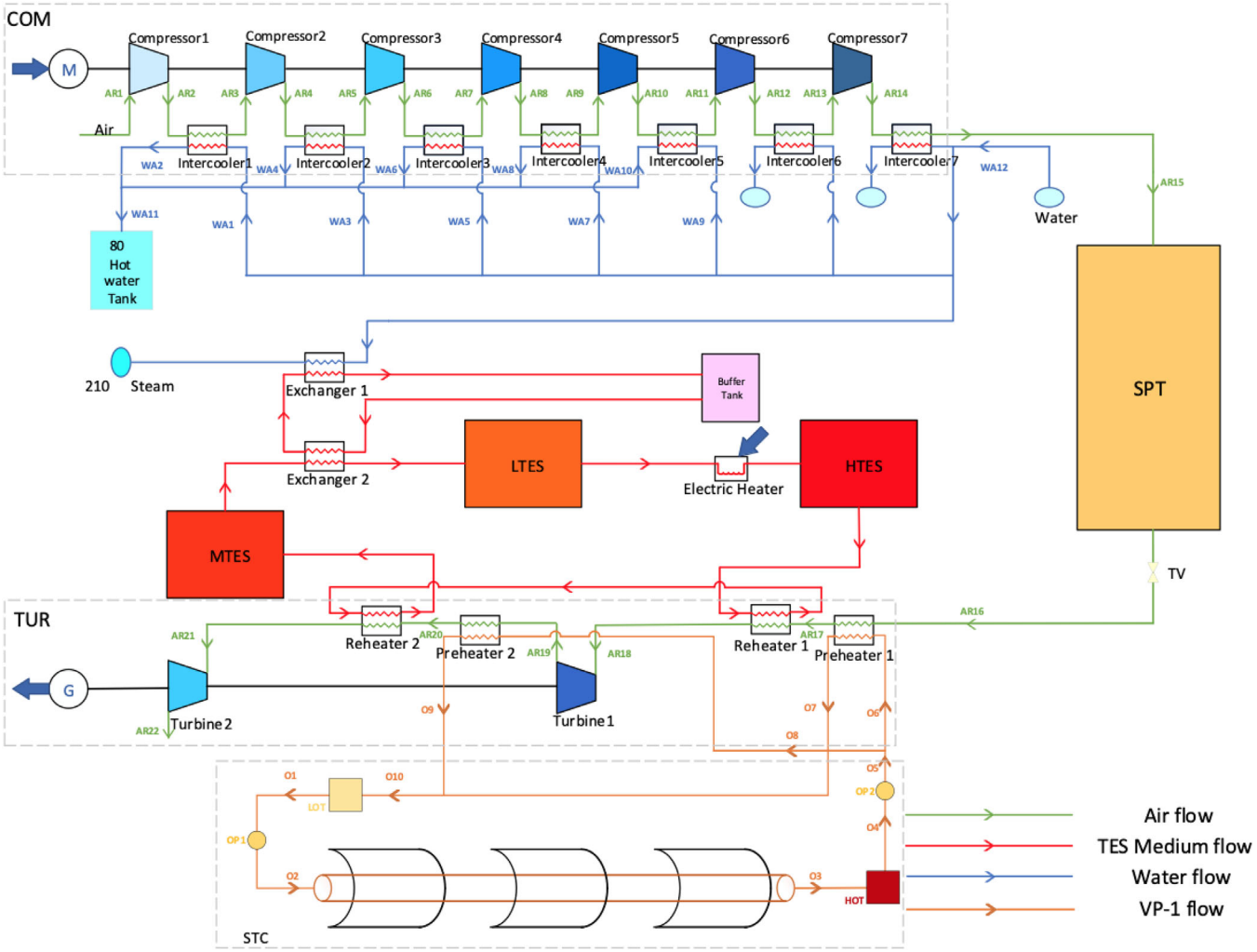

FIGURE 1 The design diagram of ST-AA-CAES.

are similar with the AA-CAES presented in previous research [9, 15–17], ST-AA-CAES has two obvious characteristics. First, the solar energy can be collected to preheat the high-pressure air to achieve a set temperature. Second, the preheating provided by the solar energy can reduce the power consumption of the MSTS system to improve the overall efficiency.

3 | MATHEMATICAL MODEL FOR THERMODYNAMIC AND EXERGY ANALYSIS

3.1 | Model assumptions

The performance index using the first law of thermodynamics can achieve energy conversion in the system. However, the efficiency evaluation index can only realize the quantitative relationship of energy utilization in the system, but the difference in energy utilization grade is difficult to be realized and applied to the analysis of the multi-energy supply of AA-CAES. Moreover, the exergy efficiency index using the second law of thermodynamics was defined to evaluate the system performance [18].

The ST-AA-CAES system combines two subsystems: first, AA-CAES; second, STC. To analysis the system, state Robinson equation should be chosen as the medium and Thermoflow software was used for analysis. To simplify the analysis, the hypothesises are as follows:

1. Air is an ideal gas and follows the ideal gas state equation
2. The heat capacity between air and heat transfer medium is constant
3. The energy loss for subsystems is not considered

3.2 | Thermodynamic model of ST-AA-CAES

The energy analysis of the ST-AA-CAES under the first law of thermodynamics. It demonstrates the coupling of various components and the energy conversion process [5]. The outlet

temperature of the compressor $T_{c,i}^{out}$ is followed by:

$$T_{c,i}^{out} = T_{c,i}^{in}\left(1+\frac{1}{\eta_{com,i}}\left(\beta_{c,i}^{\frac{k-1}{k}}-1\right)\right), \tag{1}$$

where $\eta_{com,i}$ represents the adiabatic efficiency of the i-th stage of the compressor, $\beta_{c,i}$ is the i-th stage of the compressor pressure ratio and k is the adiabatic index, and which is estimated by

$$\eta_{com,i} = \frac{h_{out,s}-h_{in}}{h_{out}-h_{in}}, \tag{2}$$

where h_{in} and h_{out} are outlet and inlet enthalpy, respectively. The power consumption of a seven-stage compressor can be obtained by

$$W_{com} = \sum_{i=1}^{7} m_{ARin}\left(h_{out}^{i}-h_{in}^{i}\right), \tag{3}$$

where the mass flow of the compressor is m_{ARin}, the production of hot water and the recovery compression heat for the energy balance equation can be expressed by

$$\begin{aligned} Q_{heat} &= m_{AR}\left(h_{A\,R,in}-h_{A\,R,out}\right) \\ &= mW_{A}\left(h_{WA,out}-h_{WA,in}\right). \end{aligned} \tag{4}$$

The operating time of SPT is determined by the upper and lower limitation of air pressures

$$\tau_{ch} = \frac{\left(P_{max}-P_{0}\right)V_{SPT}}{m_{AR15}RT}, \tag{5}$$

$$\tau_{dch} = \frac{\left(P_{max}-P_{0}\right)V_{SPT}}{m_{AR16}RT}, \tag{6}$$

where the charge and discharge time are τ_{ch} and τ_{dch}, respectively, R is the gas constant of air, V_{SPT} is the volume of SPT and T is the operating temperature of SPT. Meanwhile, $T_{out}^{e,i}$ is the outlet temperature of each stage expansion that can be achieved by

$$T_{out}^{e,i} = T_{in}^{e,i}\left(1-\eta_{e}\left(1-\pi_{i}^{\frac{1-k}{k}}\right)\right), \tag{7}$$

where the expansion ratio is π, the turbine isentropic efficiency can be used as follows

$$\eta_{e} = \frac{h_{out}-h_{in}}{h_{out,s}-h_{in}}. \tag{8}$$

Similarly with the COM system, the equation of energy balance for the expansion process is

$$m_{AR10}\left(h_{ARin}-h_{ARout}\right) = m_{O}\left(h_{Oout}-h_{Oin}\right). \tag{9}$$

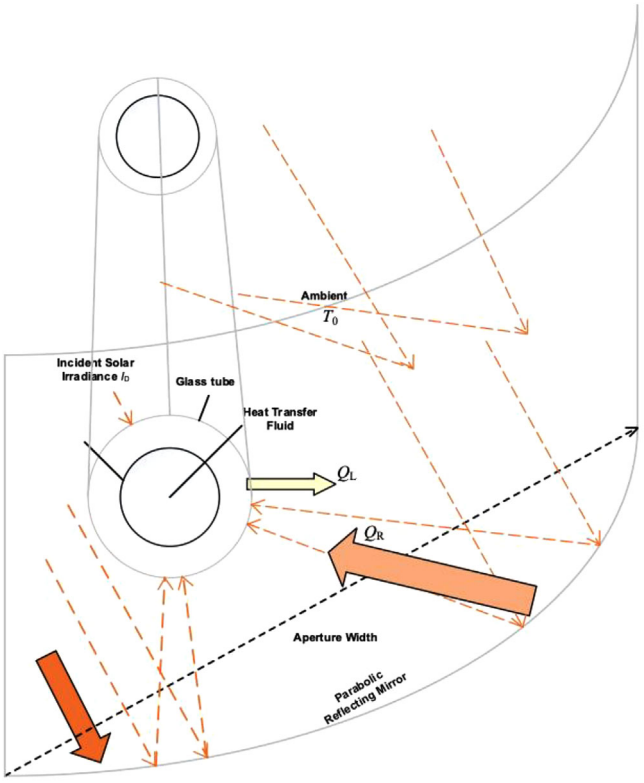

FIGURE 2 The model of Parabolic trough collection.

The power generation of a two-stage turbine can be obtained by

$$W_{Tur} = \sum_{j=1}^{2} m_{AR10}\left(h_{out}^{j}-h_{in}^{j}\right). \tag{10}$$

3.3 | STC

Figure 2 demonstrates the operation of STC is the utilization of the trough collector to collect solar radiation energy, and then heating the thermal oil in the LOT for preheating the high-pressure air released from the SPT through TV. The temperature of high-pressure air can be determined by the energy balance [19, 20], as follows

$$\eta_{C} = \frac{Q_{u}}{Q_{s}}, \tag{11}$$

where Q_s is the incident energy which is proportional to the PTC area per unit collector area and direct normal insolation, and is estimated by

$$Q_{s} = I_{D}A, \tag{12}$$

where the direct normal exposure is I_D and the surface of effective collection is A, a portion of the solar energy is transmitted

to the receiver as a function of the optical efficiency of the parabolic trough mirror [21]. The expression of the relation between optical efficiency and incident energy is shown below

$$Q_R = \eta_{op} Q_s, \tag{13}$$

where the efficiency of optical is η_{op}, the effective thermal energy collection can be calculated by

$$Q_u = Q_R - Q_L. \tag{14}$$

The effective heat absorbed by the absorber can be obtained by subtracting its heat loss. Under ordinary circumstances, it consists of different kinds of heat dissipation such as conduction, convection and radiation [22]. Moreover, the equation of heat loss can be demonstrated by

$$Q_L = Q_{cond} + Q_{conv} + Q_{rad}. \tag{15}$$

The heat conduction loss between the glass tube is neglected with simplification on the analysis of glass cladding and absorption tube thickness [23]. The thermal loss of each layer can be illustrated as

$$\begin{aligned} Q_{conv} &= Q_{conv1,2} + Q_{conv2,0}, \\ Q_{conv1,2} &= h_d (T_1 - T_2) A_{Qab}, \\ Q_{conv2,0} &= h_c (T_2 - T_0) A_g, \end{aligned} \tag{16}$$

where the thermal convective consumption between the surface of absorber tube and the inner glass tube is $Q_{conv1,2}$, the thermal convection loss between the inner glass tube and the outer environment is $Q_{conv2,0}$. A_{ab} and A_g are the absorber surface and glass tube surface, respectively. h_d is the convective heat transfer coefficient of the heat collection pipe, h_c is heat transfer coefficient between glass tube and environment, T_1 and T_2 are the surface temperatures of the absorption tubes and glass tubes, respectively.

$$Q_{rad} = Q_{rad1,2} + Q_{rad2,0}. \tag{17}$$

According to the operating characteristics of the PTC, external tube has higher temperature than glass tube and their direct thermal radiation should be considered

$$Q_{rad1,2} = \frac{\sigma \left(T_1^4 - T_2^4\right)}{\frac{1}{\varepsilon_1} + \frac{(1-\varepsilon_2)D_1}{\varepsilon_2 D_2}} A_{ab}, \tag{18}$$

where the Stefan-Boltzmann constant is σ, diameters of the outer and inner glass tube are D_1 and D_2, respectively. T_1 and T_2 are the external surface and inner glass tube surface temperatures of the receiver. ε_1 and ε_2 are the emissivity of the chosen coating and glass tube. The thermal radiation can be defined as

$$Q_{rad2,0} = \sigma \varepsilon_2 \left(T_2^4 - T_0^4\right) A_g. \tag{19}$$

The modelling of three tanks depends on dynamic mass balance and dynamic energy balance scheme which can be achieved by the following equation [18]

$$\rho_{HTF} \frac{dV_{HTF}}{dt} = m_{in} - m_{out}, \tag{20}$$

where the volume of HTF in the tank is V_{HTF}, the density of HTF is ρ_{HTF}. Meanwhile, the energy balance can be expressed by

$$\begin{aligned} \rho_{HTF} C_{HTF} \frac{d(V_{HTF} T)}{dt} &= C_{HTF} (T_{in} m_{in} - T m_{out}) \\ &- \mathcal{U} A_t (T - T_0), \end{aligned} \tag{21}$$

where $\mathcal{U}$ and A_t are the heat transfer coefficient and the surface of the heat-transfer tank, respectively. Since the volume of HTF is not constant, it is hypothesized that heat transfer cannot lead to the heat transfer for the whole tank. To further illustrate the energy balance for the HTF, the details of the PTC parameters are listed in Table 1.

TABLE 1 Rated parameters of PTC [26].

Parameters of PTC	Data
Optical efficiency	75%
Length of reflector (m)	64.15
Rows number	10
Aperture width (m)	2
Specular reflectivity	0.93
Emissivity of absorber tube	0.15
Type of mirror	White float glass

Under certain solar irradiation conditions, the thermal energy collected based on the main design components (field area and optical efficiency of the mirror) increases with the increasing of mirror field area [24]. The optical efficiency is affected by the transmittance of the glass envelope, optical intercept factor and cosine loss correction. In the meantime, the cosine loss correction factor is related to the tracking accuracy [25]. So as the efficiency of optical increases, the efficiency of thermal collection also increases.

Exergy analysis and exergy destruction are adopted the above the thermodynamic model of ST-AA-CAES, SPT model and second principle of thermodynamics for overall and each subsystem. In general, the exergy of enthalpy h can be formulated by

$$E x_i = m_i \left[(h_i - h_0) - T_0 (s_i - s_0)\right], \tag{22}$$

where m is the mass flow rate, s is the entropy of flow, i and o are state and ambient conditions, respectively. The thermal exergy supplied by the compression heat can be estimated as follow

$$E\,x_{heat} = Ex_{WA11} - Ex_{WA12}. \tag{23}$$

The exergy supply for TUR can be expressed by

$$E\,x_{HTF} = Ex_{O5} - Ex_{O10}. \tag{24}$$

3.4 | Performance criteria

There are two types of operating modes for the proposed ST-AA-CAES: energy storage and energy release. Compared to the traditional CAES, the operating mode includes the storage of electric through compressed air, preheating the molten slat and solar energy to store heat. Solar heat collection and storage and MSTS can be operated independently. Therefore, the processes of operating modes can be processed simultaneously. When the demand side needs energy, the high-pressure air in the SPT should be preheated by the PTC and then heated by the HOT system to reach the expected temperature to drive the turbine for the power generation. The heat energy is directly provided by the TES system such as 80°C hot water, 210°C industrial steam and heating suppler. Where E2E can be described as

$$\eta_{ESE} = \frac{W_{TUR}}{W_{COM}}. \tag{25}$$

In the complete charging and discharging cycle mode – RTE, the total heat and energy production of turbine are taken as the numerator and the energy consumption of the compressor and heat storage of molten salt are taken as the denominator. The equation can be expressed as follows

$$\eta = \frac{W_{TUR} + Q_c + Q_{heat}}{W_{COM} + E_{TES}}, \tag{26}$$

where Q_c is the cooling energy from the expansion process. The exergy efficiency can be depicted by

$$\eta_{EXE} = \frac{W_{TUR} + Ex_{heat} + Ex_c}{W_{COM} + Ex_{HTF}}, \tag{27}$$

where Ex_c is the cooling exergy supplied by the energy exchange between ambient temperature and outlet temperature of last stage turbine. For each subsystem j, output exergy of turbine and exergy of external heating are included in the molecular part and the denominator is the exergy of compressor consumption and exergy of heat absorbed by HTF in the compressed AST. The exergy destruction and exergy efficiency can be estimated as follows:

TABLE 2 Equations of exergy flow.

Subsystem	Ex_{in}	Ex_{out}
AC	$W_{COM} + Ex_{AR3} + Ex_{AR5} + Ex_{AR7} + Ex_{AR9} + Ex_{AR11} + Ex_{AR13}$	$Ex_{AR2} + Ex_{AR4} + Ex_{AR6} + Ex_{AR8} + Ex_{AR10} + Ex_{AR12} + Ex_{AR14}$
HEX of COM	$Ex_{AR2} + Ex_{AR4} + Ex_{AR6} + Ex_{AR8} + Ex_{AR10} + Ex_{AR12} + Ex_{AR14} + Ex_{WA1} + Ex_{AR3} + Ex_{WA5} + Ex_{WA7} + Ex_{WA9}$	$Ex_{AR3} + Ex_{AR5} + Ex_{AR7} + Ex_{AR9} + Ex_{AR11} + Ex_{AR13} + Ex_{WA2} + Ex_{WA4} + Ex_{WA6} + Ex_{WA8} + + Ex_{WA10}$
STC	Ex_{Qu}	$Ex_{O3} - Ex_{O2}$
AT	$Ex_{AR18} + Ex_{AR21}$	$W_{TUR} + Ex_{AR19} + Ex_{AR22}$
HEX of TUR	$Ex_{AR16} + Ex_{AR17} + Ex_{AR19} + Ex_{AR20} + Ex_{O5}$	$Ex_{AR17} + Ex_{AR18} + Ex_{AR20} + Ex_{AR21} + Ex_{O10}$
SPT	Ex_{AR15}	Ex_{AR16}

The energy loss for each subsystem is

$$L_j = E_{j,in} - E_{j,out}, \tag{28}$$

$$\eta_{EXE,j} = \frac{E_{j,out}}{E_{j,in}}. \tag{29}$$

The exergy flows of subsystem and designed parameters of the ST-AA-CAES are provided in Tables 2 and 3, respectively. Table 4 shows that the compression ratio of each stage of compressor and the expansion ratio of each stage of turbine.

4 | PSO OF CER

Based on the above exergy analysis, the proposed ST-AA-CAES system can be acted as the CER. To simplify the process of calculation of CER, the cooling energy rarely can be ignored in the calculation of optimal economics. The CER economic dispatch (CERED) problem combining heat and power and economic dispatch (ED) is a challenging non-convex and nonlinear optimization problem, it is necessary to consider that meet the demand of the power and thermal output of the system to minimize operating costs [27].

In previous research, different mathematical models and approaches were adopted for the CERED. For example, the CERED was decomposed into a sub-problem constrained by two operating regions which are the demand for thermal and power [28]. The proposed approach of Lagrange can be utilized to mitigate the optimization problem and implement the various heuristic method. At the same time, a penalty function

TABLE 3 Parameters of the ST-AA-CAES system.

Parameters	Value
The stage of compression	7
The stage of expansion	2
Compressor isentropic efficiency, $\eta_{c,i}$	0.84
Turbine isentropic efficiency, $\eta_{e,i}$	0.9
Air mass flow of compressor, t/h	26.6
Air mass flow of turbine, t/h	52.05
Air mass flow of thermal storage medium, t/h	36.97
Specific heat capacity of air at constant pressure, J/kg·**k**	1005
The specific heat capacity of water, J/kg·**k** Air constant, J/kg·**k**	4200 287
Heat transfer coefficient between air and the outside of the tank, $W/(m^2 \cdot k)$	30
The operation of STC, h	4
80°C Hot water supply, h	8
210°C Industrial steam supply, h	16
Heat collection efficiency, %	66.8
Ambient temperature, k	293
Environment pressure, MPa	0.1
Air storage pressure, MPa	10

TABLE 4 Parameters of each stage of compressor and turbine.

Stage	Compressor Compression ratio, β	Turbine Expansion ratio, π
1	2.41	4.47
2	1.98	8
3	1.98	
4	1.98	
5	1.98	
6	1.97	
7	1.92	

formula of the genetic algorithm proposed in [29] is improved to further reduce the error by the utilization of the variance of the preceding term. PSO was originally developed to graphically simulate the graceful and unpredictable movements of a bird flock. Though observing the social behaviour of animals and finding the social sharing of information in groups to provide an evolutionary advantage which is used as the developing basis for algorithms [30]. In this section, PSO is adopted to achieve the optimal results.

4.1 | Application of PSO to CER

PSO is widely used to solve different power system problems [31]. To find the appreciate fitness values through random numbers, it based on the objective function and the process of all evolutionary algorithms by the generation of random numbers. In the meanwhile, the position of a particle as a decision variable in PSO can be expressed by position vector X and a velocity vector V in each iteration, the equations as follow

$$X_i^{iter} = \left[x_{i,1}^{iter}, x_{i,2}^{iter}, \ldots, x_{i,N}^{iter}\right], \tag{30}$$

$$V_i^{iter} = \left[v_{i,1}^{iter}, v_{i,2}^{iter}, \ldots, v_{i,N}^{iter}\right], \tag{31}$$

where N is the total number of decision variables, and the operating principle of iteration is that each particle in each iteration uses its current speed and the experience of other particles to achieve a better position. The mathematical equations can be estimated by

$$v_n^{iter} = \omega \times v_n^{iter-1} + c_1 \times r_1^n \times \left(p_{best_{i,n}}^{iter-1} - x_{i,n}^{iter-1}\right) + c_2 \times r_2^n \times \left(g_{best_{i,n}}^{iter-1} - x_{i,n}^{iter-1}\right), \tag{32}$$

$$x_{i,n}^{iter} = x_{i,n}^{iter-1} + v_{i,n}^{iter}, \tag{33}$$

where the inertia coefficient is ω, r_1^n and r_2^n are the interval [0, 1] for random numbers, $p_{best_{i,n}}^{iter-1}$ and $g_{best_{i,n}}^{iter-1}$ are the best position of ith particle in previous iteration and entire swarm, respectively. The learning components are c_1 and c_2. The predefined range for updated velocities is as follow

$$-v_n^{min} \le v_{i,n} \le v_n^{max}, \tag{34}$$

$$v_n^{max} = \left(x_n^{max} - x_n^{min}\right) / r, \tag{35}$$

where x_n^{min} and x_n^{max} are the minimum and maximum limits of variables, r is a component for the control of velocity value.

Figure 3 illustrates the application of PSO to the CERED problem and the principle of an evolutionary algorithm to verify the effectiveness of this approach in the power system.

4.2 | PSO-based on CER optimization model

In CER there are three different conditions of operation, including power-only, combining heat and power units and heat-only units.

4.2.1 | Constraints

The constraints based on demand for power and heat of the system are as follows

$$\sum_{v=1}^{N_p} P_v^p + \sum_{n=1}^{N_c} P_{\chi}^c = P_d + P_{loss}, \tag{36}$$

$$\sum_{n=1}^{N_c} H_{\chi}^c + \sum_{k=1}^{N_h} H_k^h = H_d, \tag{37}$$

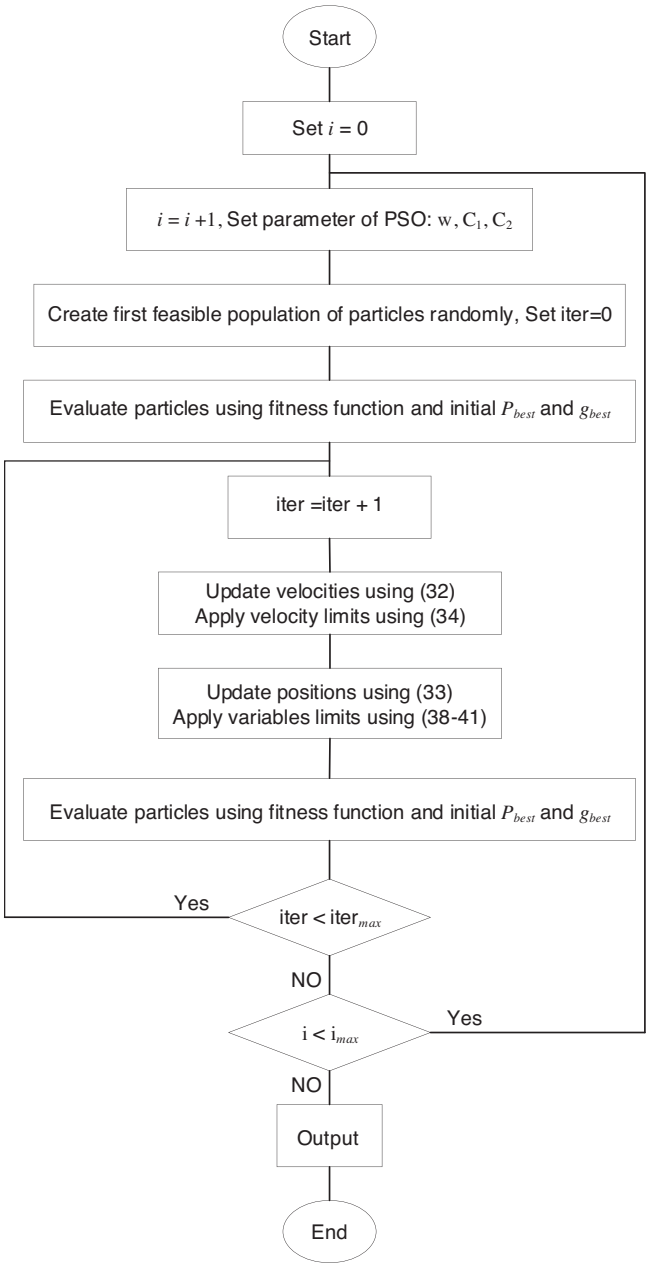

FIGURE 3 Diagram of implementing PSO into CER [32

where the demand for power and heat are P_d and H_d, respectively. P_{loss} is the transmission loss of the power system. The operating regions of different units should be limited by

$$P_v^{pmin} \le P_v^p \le P_v^{pmax} \quad v = 1, 2, 3, \dots, N_p, \tag{38}$$

$$P_z^{cmin} \le P_z^c \le P_z^{cmax}\left(H_z^c\right), z = 1, 2, 3, \cdots, N_c, \tag{39}$$

$$H_z^{cmin}\left(P_z^c\right) \le H_z^c \le H_z^{cmax}\left(P_z^c\right), z = 1, 2, 3, \cdots, N_c, \tag{40}$$

$$H_k^{hmin} \le H_k^h \le H_k^{hmax}, k = 1, 2, 3, \cdots, N_h. \tag{41}$$

For power-only units, P_v^{pmin} and P_v^{pmax} are the limitations of lower and upper generation, respectively. The range of power and heat outputs of combining heat and power units are P_z^{cmin}, P_z^{cmax}, H_z^{cmin} and H_z^{cmax}, respectively. H_k^{hmin} and H_k^{hmax} are limits for heat-only units.

The system can be regarded as compositing of three parts, including power-only units, cogeneration units and heat-only units. To simplify the process of calculation, the transmission loss of the system can be ignored. Based on the demand for the power and heat are 20 MW and 83.66MW, the cost functions of them are linear as follow

$$C_1\ (P_1) = 12.5P_1; 0 \le P_1 \le 37.5, \tag{42}$$

$$C_4\ (H_4) = 23.4H_4; 0 \le H_4 \le 1957.7. \tag{43}$$

4.2.2 Objective function

The objective function of CER should be determined to minimize the operation cost.

$$OBJ = \sum_{v=1}^{N_p} C_v\left(P_v^p\right) + \sum_{n=1}^{N_c} C_z\left(P_z^c, H_z^c\right) + \sum_{k=1}^{N_k} C_k\left(H_k^h\right), \tag{44}$$

where the operation cost of the power-only unit for generating P_v^p MW is $C_v(P_v^p)$, the operation cost of combining heat and power units (power: P_z^c MW and heat: H_z^c) is $C_z(P_z^c, H_z^c)$, the operation cost of heat-only units (H_k^h) is $C_k(H_k^h)$ MW. N is the number of each type of unit, v, z and k are indices for each type of unit, respectively. The cost functions of each type of unit can be estimated by [32]

$$C_v\left(P_v^p\right) = \alpha_v\left(P_v^p\right)^2 + \beta_v P_v^p + \gamma_v\left(\frac{\$}{h}\right), \tag{45}$$

$$C_z\left(P_z^c, H_z^c\right) = a_z\left(P_z^c\right)^2 + b_z P_z^c + c_z + d_z\left(H_z^c\right)^2 + e_z H_z^c + f_z P_z^c H_z^c\left(\frac{\$}{h}\right), \tag{46}$$

$$C_k\left(H_k^h\right) = a_k\left(H_k^h\right)^2 + b_k H_k^h + c_k\left(\frac{\$}{h}\right), \tag{47}$$

where α_v, $\beta_v$and γ_v are coefficients of cost function related to power-only units. a_z, b_z, c_z, d_z, e_z and f_z are cost coefficients for combining heat and power units. a_k, b_k and c_k are cost coefficients for heat-only units.

TABLE 5 Simulation results of the ST-AA-CAES system in typical operating conditions.

Parameters	Data
MSTS mass flow (kg/s)	36.97
VP-1 mass flow (kg/s)	8.52
Water mass flow (kg/s)	2.27
E2E (%)	56.4
RTE (%)	95.5
Exergy efficiency (%)	55.9
Power consumption of compression (kW)	4315
Power generation of expansion (kW)	2436
PTC power collection (kW)	2122

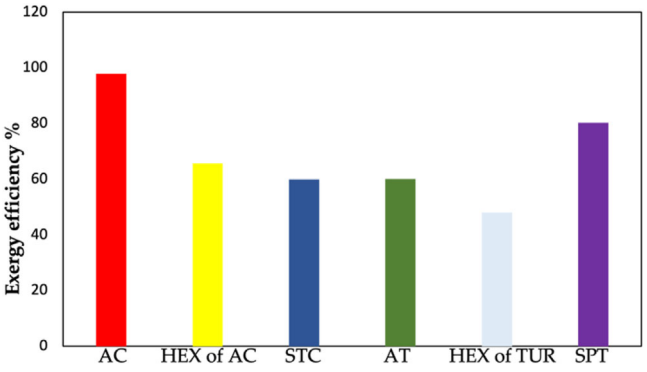

FIGURE 4 Exergy efficiencies of each subsystem.

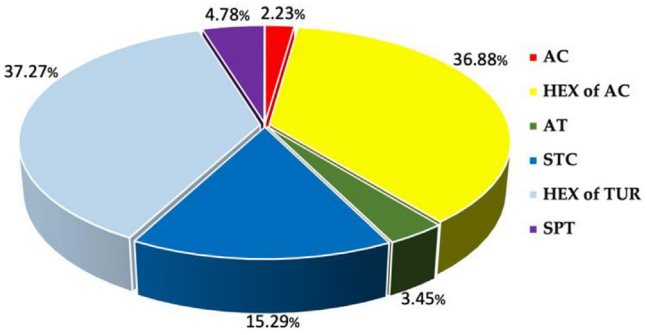

FIGURE 5 Exergy destruction of each subsystem.

5 | NUMERICAL RESULTS

5.1 | Exergy analysis

For exergy analysis, Table 5 illustrates the key simulation results of the ST-AA-CAES system in typical operating scenarios. At the same time, the flow parameters of air, oil (Therminol VP-1) and water are listed in Tables 6 and 7, respectively. Based on the parameters from the above table, E2E, RTE and exergy efficiency of the system are 56.4%, 95. 5%, and 55.9%, respectively. The temperature of water increases from 15.01°C to 80°C. STC needs about 4 h to increase the temperature of VP-1 from 105.3°C to 250°C under the average situation. Since the efficiency of the expansion generator depends on the temperature of the high-pressure air, it is critical for the VP-1 temperature given by the solar energy absorped and stored. The performance improvement of ST-AA-CAES mainly depends on two key technologies: first, utilize TES to store the compression heat through the water medium and use abandon power to heat molten salt to store the heat; second, the utilization of STC to store the solar heat VP-1 medium. Efficient storage and utilization of compression heat can improve the power generation efficiency and meet the thermal energy demand for users, such as hot water and user thermal supply etc.

Based on the above data in Tables 6 and 7 with formulas (27) and (28), the performance of each subsystem in CER can be analysed for exergy destruction and efficiency. The exergy efficiencies of all subsystems are provided in Figure 4. The exergy efficiency of STC is lower than the rest subsystems due to its basic characteristics such as some internal factors (optical efficiency, mass flow, mirror field area etc.) and external factors (weather: rainy and cloudy day) [33]. In addition, the enthalpy efficiency of HEX of TUR and AT is relatively low because of the high-temperature difference during the discharge process of high-pressure air.

Figure 5 depicts the exergy destruction in the CER system. The exergy destruction of the STC system is 15.29%, which is due to external heat conduction, convection and radiation from the parabolic mirror surface and absorption tube leads to many irreversible losses during the operation of the STC [34]. Because it spends a long period to achieve the design temperature, therefore, exergy destruction of the STC during this process can be ignored in the overall analysis. Because of the irreversible heat loss of the process of heat transfer, HEX of TUR and HEX of AC have relatively more exergy destruction of the CER.

Some main simulation results can be compared between AA-CAES in [5] and hybrid adiabatic compressed air energy storage (HA-CAES) in Table 8. First, the RTE and EXE for each system are 95.5% and 55.9%, respectively. The main difference with ST-AA-CAES is that the STC can be implemented as an additional subsystem to collect and store the solar energy in comparison with the AA-CAES system. For the HA-CAES system, the main difference with ST-AA-CAES is that TES is not included with the output power of the air turbine and should be affected by the change of solar radiation. Although the HA-CAES system has relatively higher exergy efficiency, it depends on the fuel combustion of fossil fuel which could cause environment and air pollution, it is contrary to the development of zero carbon emission in the current world. Compared to the above ST-AA-CAES and HA-CAES systems, ST-AA-CAES not only store compression heat through the TES to improve the power generation efficiency and thermal supply, but it also collects the solar energy though the STC system to reduce power consumption in the MSTS system and further enhance the overall efficiency and flexibility.

TABLE 6 The thermodynamic analysis results of air.

Stream	T (°C)	P (MPa)	h (kJ/kg)	s (kJ/kg.k)	Ex (kJ/kg)	m (kg/s)
AR1	20	0.0995	419.41	3.8687	0.00	7.39
AR2	120	0.24	520.14	3.9116	88.17	7.39
AR3	40	0.2182	439.29	3.7090	66.69	7.39
AR4	120	0.4315	519.92	3.7425	137.50	7.39
AR5	40	0.411	438.90	3.5261	119.92	7.39
AR6	120	0.8134	519.47	3.5592	190.79	7.38
AR7	40	0.7747	438.15	3.3420	173.16	7.34
AR8	120.1	1.532	518.75	3.3753	243.99	7.34
AR9	40	1.459	436.87	3.1565	226.24	7.32
AR10	120	2.882	517.15	3.1890	296.98	7.32
AR11	40	2.771	434.18	2.9644	279.88	7.31
AR12	120	5.465	514.48	2.9969	350.62	7.31
AR13	40	5.306	429.40	2.7634	334.00	7.30
AR14	121	10.2	511.28	2.8061	403.36	7.30
AR15	40	10	421.36	2.5563	386.68	7.30
AR16	40	4	431.82	2.8519	310.49	14.46
AR17	150	4	547.29	3.1680	333.28	14.46
AR18	200	3.846	704.62	3.4976	393.99	14.46
AR19	124.8	0.8614	524.31	3.5550	196.97	14.46
AR20	150	0.8614	550.04	3.6177	204.23	14.46
AR21	200	0.8204	601.35	3.7463	217.83	14.46
AR22	10	0.1025	409.34	3.8252	2.67	14.46

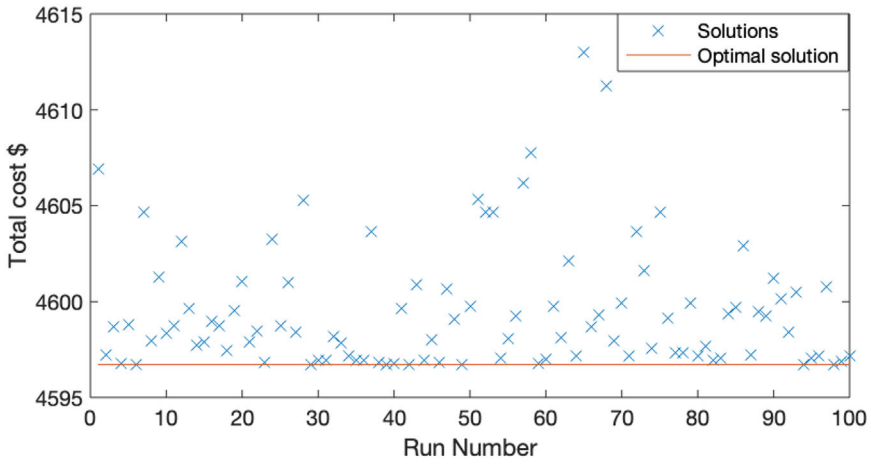

FIGURE 6 Variety solutions and optimal result of PSO.

5.2 | Effectiveness of PSO for ST-AA-CAES (variables of decision variables should also be given)

To verify the accuracy of the approach proposed in Section 4, it was set to run 100 times for the random nature of evolutionary is depicted in Figure 6. Based on the demand for heat (83.66MW) and power (20MW) as constraints, the results illustrate that the optimal cost of the system is 4596.87$. Figure 7 illustrates the good performance of convergence in this algorithm to further clarify the feasibility of the system. Table 9 demonstrates the optimal results and variance of all results for this combining heat and power system.

Table 9 depicts that the variables cost results based on the different kind of sensitivity situations. To satisfy the practical requirements, more reasonable test conditions are considered to further support the proposed method. The results deliver a message that our method is solid and could be widely applied to industrial society.

TABLE 7 The thermodynamic analysis result of water and Therminol VP-1.

Stream	T (°C)	P (MPa)	h (kJ/kg)	s (kJ/kg.k)	Ex (kJ/kg)	m (kg/s)
WA1	15.01	0.52	412.53	3.3634	0.00	2.18
WA2	80	0.40	478.67	3.6456	-15.19	2.18
WA3	15.01	0.52	412.53	3.3634	0.00	2.27
WA4	80	0.40	478.67	3.6456	-15.19	2.27
WA5	15.01	0.52	412.53	3.3634	0.00	2.52
WA6	80	0.40	478.67	3.6456	-15.19	2.52
WA7	15.01	0.52	412.53	3.3634	0.00	2.35
WA8	80	0.40	478.67	3.6456	-15.19	2.35
WA9	15.01	0.52	412.53	3.3634	0.00	2.27
WA10	80	0.40	478.67	3.6456	-15.19	2.27
WA11	80	0.40	478.67	3.6456	-15.19	11.69
WA12	15	0.40	412.86	3.4396	-21.65	14.58
O1	105.3	0.1014	0.1009	-2.754	11.72	8.52
O2	105.6	0.4372	0.787105	-2.75278	12.14	8.52
O3	250	0.1014	243.1709	-2.21482	94.12	8.52
O4	250	0.24	243.2409	-2.21499	94.24	8.52
O5	250	0.1034	243.1719	-2.21482	94.13	8.52
O6	250	0.1014	243.1719	-2.21482	94.13	6.9
O7	100	0.1034	-7.2053	-2.77313	10.21	6.9
O8	250	0.1014	243.1719	-2.21482	94.13	1.62
O9	127.6	0.1034	32.09951	-2.67157	19.23	1.62
O10	105.3	0.104	0.102984	-2.75369	11.72	8.52

FIGURE 7 Convergence of PSO for the optimal solution.

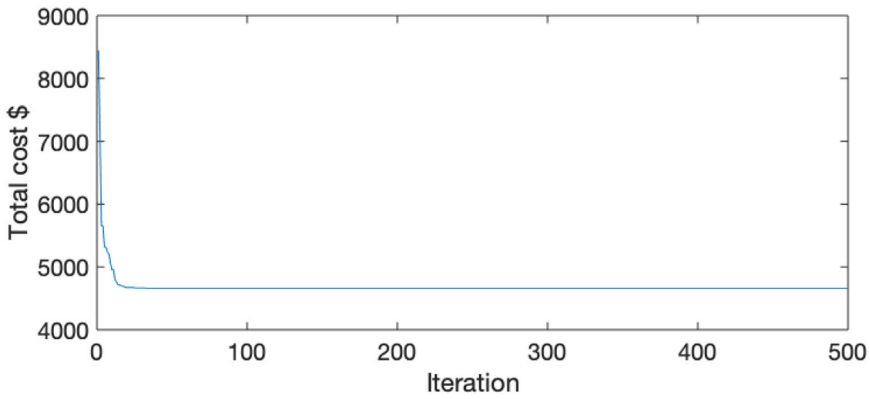

TABLE 8 The comparison of performance of ST-AA-CAES.

Parameters	Unit	ST-AA-CAES	AA-CAES	Hybrid A-CAES
With/without TES	/	Yes	Yes	No
Inlet temperature of air turbine	°C	300	300	900
E2E	%	56.4	56.4	/
RTE	%	95.5	93.6	87
Exergy efficiency	%	55.9	/	80

6 | CONCLUSION

The CER based on the ST-AA-CAES provides the operating opportunity of combining cooling, thermal and power for multiple forms. To further utilize the natural energy, the ST-AA-CAES has been proposed in this paper and implemented in the STC system. The high-pressure air from SPT is preheated by stable solar thermal energy and then reheated by the MSTS system, which further enhances the performance of ST-AA-CAES and the generation efficiency of power. The compression heat from the HEX of COM can be used to supply 8-h of 80°C

TABLE 9 The variable results based on sensitivity situations.

Case	Changes in power (P) and heat (H) demand	Data ($)
1	P (95%) and H (95%)	4543.97
2	P (95%) and H (100%)	4592.11
3	P (95%) and H (105%)	4641.44
4	P (100%) and H (95%)	4549.31
5	P (100%) and H (100%)	4596.87
6	P (100%) and H (105%)	4643.56
7	P (105%) and H (95%)	4554.63
8	P (105%) and H (100%)	4602.39
9	P (105%) and H (105%)	4651.77

hot water and the cooling energy from the expansion process can be collected for a 4-h cooling energy supply. In addition, 16-h of 210°C industrial steam is supplied by the MSTS. ST-AA-CAES mainly consists of a seven-stage compression and a two-stage expansion to establish a mathematical model of energy and exergy analysis, the E2E, RTE and exergy efficiency are 56.4%, 95.4%, 55.9%, respectively. Meanwhile, for the investigation of the economy, PSO can be applied to the analysis and optimize the integrated energy system, and the optimal result is 4596.87$. This work provides a guidance for further optimization and economic analysis of ST-AA-CAES and a scheme for the energy management of ambient wind and solar power.

AUTHOR CONTRIBUTION

Chenyixuan Ni: Conceptualization, data curation, investigation, methodology, software, validation, writing - original draft. **Laijun Chen**: Investigation, validation, writing - review & editing. **Xiaotao Chen**: Conceptualization, methodology, software, validation, writing - review & editing. **Junyi Zhai**: Methodology, writing - review & editing. **Shengwei Mei**: Funding acquisition, supervision, writing - review & editing. **Xiaoping Zhang**: Funding acquisition, methodology, software, supervision, writing - review & editing.

CONFLICT OF INTEREST STATEMENT

The authors declare no conflict of interest.

DATA AVAILABILITY STATEMENT

Data available on request from the authors.

ORCID

Xiao-Ping Zhang https://orcid.org/0000-0003-0995-4989

REFERENCES

1. Aldaadi, M., AI-Ismail, F., AI-Awanmi, A., et al.: A Coordinated bidding model for wind plant and compressed air energy storage systems in the energy and ancillary service markets using a distributionally robust optimization approach. IEEE Access 9, 148599–148610 (2021)
2. Krupke, C., Wang, J., Clarke, J., et al.: Modelling and experimental study of a wind turbine system in hybrid connection with compressed air energy storage. IEEE Trans. Energy Conver. 32, 137–145 (2017)
3. Bhattarai, S., Karki, R., Piya, P.: Reliability modelling of compressed air energy storage for adequacy assessment of wind integrated power system. IEEE Gener. Transm. Distrib. 4, 4443–4450 (2019)
4. Ji, W., Zhou, Y., Sun, Y., et al.: Thermodynamic analysis of a novel hybrid wind-solar-compressed air energy storage system. Energy Convers. Manage. 142, 176–187 (2016)
5. Ni, C., Xue, X., Mei, S., et al.: Technological research of a clean energy router based on advanced adiabatic compressed air energy storage system. Entropy 22, 1440 (2020)
6. Luo, X., Wang, J., Dooner, M., et al.: Overview of current development in electrical energy storage technologies and the application potential in power system operation. Appl. Energy 137, 511–536 (2015)
7. Cleary, B., Duffy, A., OConnor, A., et al.: Assessing the economic benefits of compressed air energy storage for mitigating wind curtailment. IEEE Trans. Sustain. Energy 6, 1021–1028 (2015)
8. Guo, Z., Wei, W., Chen, L., et al.: Operation of distribution network considering compressed air energy storage unit and its reactive power support capability. IEEE Trans. Smart Gird. 11, 2954–2965 (2020)
9. Mozayeni, H., Negnevitsky, M., Wang, X., et al.: Performance study of and advanced adiabatic compressed air energy storage system. Energy Procedia 110, 71–76 (2017)
10. Morteza, S.K., Seyed, M.M.N.: Thermodynamic and economic analysis of a novel combination of the heliostat solar field with compressed air energy storage (CAES); a case study at San Francisco, USA. J. Energy Storage 49, 104111 (2022)
11. Peng, R., Yue, W., Yase, W., et al.: Thermodynamic, economic and environmental investigations of a novel solar heat enhancing compressed air energy storage hybrid system and its energy release strategies. J. Energy Storage 55, 105423 (2022)
12. Shadi, B., Mousavi Pouria, A., Ali, P., Pedram, H.: A comprehensive techno-economic assessment of a novel compressed air energy storage (CAES) integrated with geothermal and solar energy. Sustain. Energy Technol. Assess. 47, 101418 (2021)
13. Mehdi, J., Mostafa, S., Alireza, S.F.: Stochastic optimal operation of a microgrid based on energy hub including a solar-powered compressed air energy storage system and an ice storage conditioner. J. Energy Storage 33, 102089 (2021)
14. Praveen, K.C., Saiid, K., Ahmad, A., Ayyoub, M.M.: Near isothermal compressed air energy storage system in residential and commercial buildings: Techno-economic analysis. Energy 251, 123963 (2022)
15. Chaaran, A., Narendhar, R., Karthikeyan, D., et al.: Can large-scale advanced-adiabatic compressed air energy storage be justified economically in an age of sustainable energy? J. Renew. Sustain. Energy 1, 033102 (2009)
16. Roncolato, J., Zanganeh, G., Jenny, P., et al.: Advanced adiabatic compressed air energy storage design and modelling accounting for turbomachinery performance. J. Phys. Conf. Ser. 2116, 012088 (2021)
17. Zhang, W., Xue, X., Liu, F., et al.: Modelling and experimental validation of advanced adiabatic compressed air energy storage with off-design heat exchanger. IET Renewable Power Gener. 14, 389–398 (2020)
18. Szablowski, L., Krawczyk, M., Badyda, K., et al.: Energy and exergy analysis of adiabatic compressed air energy storage. Energy 138, 12–18 (2017)
19. Nation, D.D., Heggs, P.J., Dixon-Hardy, D.W.: Modelling and simulation of a novel electrical energy storage (EES) reveiver for solar parabolic trough collector (PTC) power plants. Appl. Energy 195, 950–973 (2017)
20. Nabat, M.H., Soltani, M., Razmi, K., et al.: Investigation of a green energy storage system based on liquid air energy storage (LAES) and high-temperature concentrated solar power (CSP): Energy, exergy, economic, and environmental (4E) assessments, along with a case study for San Diego, US. Sustain. Cities Soc. 75, 103305 (2021)
21. Seni, L., Guler, O.F., Yilmaz, C.: Thermodynamic modelling and analysis of a solar and geothermal assisted multi-generation energy systm. Energy Convers. Manage. 239, 114186 (2021)
22. Forristall, R.: Heat Transfer Analysis and Modelling of a Parabolic Trough Solar Receiver Implemented in Engineering Equation Solver. National Renewable Energy Laboratory, Golden, CO (2003)

23. Yao, L., Xiao, X., Wang, Y., et al.: Dynamic modelling and hierarchical control of a concentrated solar power plant with direct molten salt storage. Energy 252, 123999 (2022)
24. Aravind, G., Yadav, R.K., Yadav Loganathan, C., et al.: Experimental investigation of cavity absorber in parabolic solar collector. In: 2016 International Conference on Recent Advances and Innovations in Engineering (ICRAIE), pp. 1–5. IEEE, Piscataway (2016)
25. Ktistis, P., Agathokleous, R.A., Kalogirou, S.A.: A design tool for a parabolic trough collector system for industrial process heat based on dynamic simultion. Renew. Energy 183, 502–514 (2022)
26. Zeroual, B., Moummi, A.: Design of parabolic trough collector solar field for future solar thermal power plants in Algeria. In: 2012 2nd International Symposium on Environment Friendly Energies And Applications, pp. 168–172. IEEE, Piscataway (2012)
27. Li, L., He, D., Jin, J., et al.: Multi-objective load dispatch control of biomass heat and power cogeneration based on economic model predictive control. Energies 14, 762 (2021)
28. Jadoun, V.K., Prashanth, G.R., Joshi, S.S., et al.: Optimal fuzzy based economic emission dispatch of combined heat and power units using dynamically controlled whale optimization algorithm. Appl. Energy 315, 119033 (2022)
29. Shi, B., Yan, L., Wu, W., et al.: Multi-objective optimization for combined heat and power economic dispatch with power transmission loss and emission reduction. Energy 56, 135–143 (2013)
30. Son, Y., Oh, B., Acquah, M.A., et al.: Multi energy system with an associated energy hub: A review. IEEE Access 9, 127753–127766 (2021)
31. Sohrabi, F., Jabari, F., Pourghasem, P., et al.: Combined heat and power economic dispatch using particle swarm optimization. In: Optimization of Power System Problems: Methods, Algorithms and MATLAB code, pp. 127–141. Springer International Publishing, Cham (2020)
32. Narang, N., Sharma, E., Dhillon, J.: Combined heat and power economic dispatch using integrated civilized swarm optimization and powell's pattern search method. Soft Comput 52, 190–202 (2017)
33. Farzad, J., Emad, A., Hossein, A.: Energy and exergy of heat pipe evacuated tube solar collectors. Thermal Sci. 20, 327–335 (2016)
34. Moradi, H., Mirjalily, S.A.A., Oloomi, S.A.A., et al.: Performance evaluation of a solar air heating system integrated with a phase change materials energy storage tank for efficient thermal energy storage and management. Renew. Energy 191, 974–986 (2022)

How to cite this article: Ni, C., Chen, L., Chen, X., Zhai, J., Mei, S., Zhang, X.-P.: Exergy analysis and particle swarm optimization of clean energy router based on a solar-thermal-assisted advanced adiabatic compressed air energy storage system. IET Renew. Power Gener. 1–13 (2023).
https://doi.org/10.1049/rpg2.12758